1988ApJ...333..168M

THE ASTROPHYSICAL JOURNAL, 333:168–180, 1988 October 1
© 1988. The American Astronomical Society. All rights reserved. Printed in U.S.A.

MULTIFREQUENCY OBSERVATIONS OF THE DOUBLE-NUCLEUS GALAXY MARKARIAN 266: ENHANCED SYNCHROTRON EMISSION INDUCED BY A MERGER

JOSEPH M. MAZZARELLA, RALPH A. GAUME,[1] HUGH D. ALLER, AND PHILIP A. HUGHES
Department of Astronomy, University of Michigan
Received 1988 January 20; accepted 1988 March 29

ABSTRACT

Optical CCD images and radio aperture-synthesis observations are presented for the double-nucleus galaxy Markarian 266 (NGC 5256 = I Zw 67). Although the galaxy appears optically as a disturbed system containing two active nuclei separated by 10″, multifrequency radio synthesis images with a resolution of half-power beamwidth (HPBW) = 2″ reveal the presence of three separate nonthermal continuum sources. Two of the radio components coincide with optical Seyfert 2 and low-ionization nuclear emission-line region (Liner) nuclei, while the third source lies *between* the optical nuclei. No optical counterpart to the peak in the central radio component is apparent in broad-band or Hα images.

The peculiar optical morphology and far-infrared properties as measured by *IRAS* indicate that Mrk 266 is an ongoing interaction/merger between two previously separate galaxies. A high-resolution 6 cm synthesis image (HPBW = 0.″4 × 0.″3) reveals double structure in the central radio component, and a "linear" morphology in the SW component which is similar to that found in many isolated Seyfert nuclei.

We propose that the enhanced radio emission between the nuclei of Mrk 266 is produced by synchrotron emission stimulated by the collision of two galaxies. Shocks induced by the collision and possible ongoing merger of two disk galaxies may accelerate electrons and locally enhance the magnetic field in the region between the nuclei where compression and shocking is most intense. A detailed application of Bell's cosmic-ray acceleration mechanism, assuming equipartition of energy to derive the magnetic field and electron density, successfully explains the power and spectrum of the radio source located between the nuclei of Mrk 266. A more general implication is that shock-induced synchrotron emission may be a primary mechanism responsible for findings which indicate that close galaxy pairs and mergers are more likely to be radio-loud than galaxies in other samples.

Subject headings: galaxies: individual (Mrk 266) — galaxies: interactions — galaxies: Seyfert — galaxies: structure — radiation mechanisms — radio sources: galaxies

I. INTRODUCTION

Markarian 266 (NGC 5256 = I Zw 67) appears optically as a peculiar galaxy containing two compact nuclei within a common envelope. The nuclei are separated by 10″. Zwicky (1971) first noted the peculiar double-nucleus structure of the galaxy, and Karachentsev (1972) included the object in the *Catalog of Isolated Pairs of Galaxies in the Northern Hemisphere* (K388). Early morphological and spectroscopic studies of Mrk 266 were reported by Petrosian, Saakian, and Khachikian (1978, 1979, 1980) and Petrosian (1980). The radio designation BP173 (Dixon 1970) indicates that the first radio detection of this source was reported by Bailey and Pooley (1968). Optical spectroscopy by Petrosian *et al.* (1980) showed that both nuclei exhibit Seyfert 2 properties, while Osterbrock and Dahari (1983) and Kollatschny and Fricke (1984) reclassified the NE nucleus as a Liner based on optical spectra and *IUE* spectra, respectively.

We present optical CCD images and multifrequency radio synthesis observations of Mrk 266 which reveal a complex system consisting of extranuclear optical knots and multiple radio continuum components. The results of CCD imaging and photometry are presented in § II. These observations indicate that Mrk 266 is a close pair of interacting galaxies, perhaps in the process of merging. Radio synthesis images presented in § III show the presence of a nonthermal radio source located between the nuclei of Mrk 266, in addition to emission associated with the active nuclei and extended 20 cm emission located ∼20″ to the north of the nuclei. Radio synthesis data at 20 cm, 6 cm, and 2 cm are used to produce spectral indices for the three components, and a high-resolution 6 cm synthesis image (HPBW = 0.″3 × 0.″4) reveals substructure in the central and SW radio components. In § IV we discuss possible interpretations of these data and conclude that the enhanced radio emission between the nuclei of Mrk 266 can be consistently interpreted in terms of a particle acceleration mechanism induced by a collision or ongoing merger between two galaxies. Implications of these results are also discussed in relation to the enhanced radio emission observed in other interacting systems.

II. OPTICAL IMAGING

Broad-band CCD images of Mrk 266 were obtained in 1986 April and 1987 August using the 1.3 m telescope of the McGraw-Hill Observatory equipped with an RCA CCD camera. The observations were made through *B*, *V*, and *R* interference filters, and the use of an *f*/7.5 secondary provided a scale of 0.″63 per pixel in the focal plane. Data reduction included dark frame and bias subtraction,

[1] E. O. Hulburt Center for Space Research, Naval Research Laboratory.

© American Astronomical Society • Provided by the NASA Astrophysics Data System

1988ApJ...333..168M

dividing by appropriate flat field frames, and sky subtraction using software developed by T. A. Boroson and graduate students at the University of Michigan ("Boroson Astronomical Reduction Facility"). Sky flats were obtained by median filtering all exposures taken through a particular filter on the same night. Photometric calibrations, including the appropriate filter transformations to the Johnson system, were performed using observations of defocused standard stars (Landolt 1983). Figure 1 is a calibrated contour diagram of Mrk 266 in the *B* band. The isophotes range from 19.5 to 24.5 mag per square arcsec. In order to detect faint extended emission, *B*, *V*, and *R* images were registered to within ± 0.1 pixel and co-added. A gray-scale representation of the resulting image is displayed in Figure 2. The adopted distance of Mrk 266 is 169 Mpc, using the average of the heliocentric velocities of the two nuclei, 8364 km s^{-1} (Petrosian *et al.* 1980), and correcting for the solar motion using the equation $v_{corr} = v_{helio} + 300 \sin(l) \cos(b)$ (de Vaucouleurs, de Vaucouleurs, and Corwin 1976). A value of $H_0 = 50$ km s^{-1} Mpc^{-1} is assumed throughout this paper. The centers of the nuclei are separated by 10".0, which corresponds to 8.2 kpc at a distance of 169 Mpc. Note the faint halo that extends ~ 80 kpc $\times$ 71 kpc (98" $\times$ 86"), in addition to what appears to be a giant H II region located ~ 24 kpc (30") to the SW of the nuclei. The giant H II region was also noted by Petrosian *et al.* (1980). It is interesting to note that this object has a luminosity comparable to dwarf galaxies with H II region–like spectra, suggesting that it may indeed be a galaxy which is interacting with the two major components of Mrk 266. Faint, wispy plumes, apparently tidal features, are also visible extending to the southeast of this complex system. We also point out the presence of a peculiar loop of emission that appears to terminate at a knot near the northern extremities of Mrk 266.

In order to enhance further features in the optical emission of Mrk 266, an image "derivative" is obtained by determining the differences in CCD pixel values along the northwest direction. This technique successfully enhances peaks and edges in the image that are not clearly visible in the unprocessed images. The result, displayed in Figure 3 (Plate 7), enhances a spiral or tidal feature that extends ~ 12 kpc (15") to the north, in addition to two knots located ~ 3" 2.5 kpc northwest and west of the Seyfert 2 nucleus. The blue color of the extranuclear knot located northwest of the SW nucleus suggests it is a region of active star formation. The knot to the west of the Seyfert nucleus appears as a distinct peak in an Hα image which will be discussed below. The results of synthetic aperture photometry for the nuclei, the giant H II region, and the entire system are presented in Table 1. Absolute magnitudes are calculated using the distance of 169 Mpc noted above. The Galactic extinction, $E(B-V)$, in the direction of Mrk 266 (NGC 5256) is

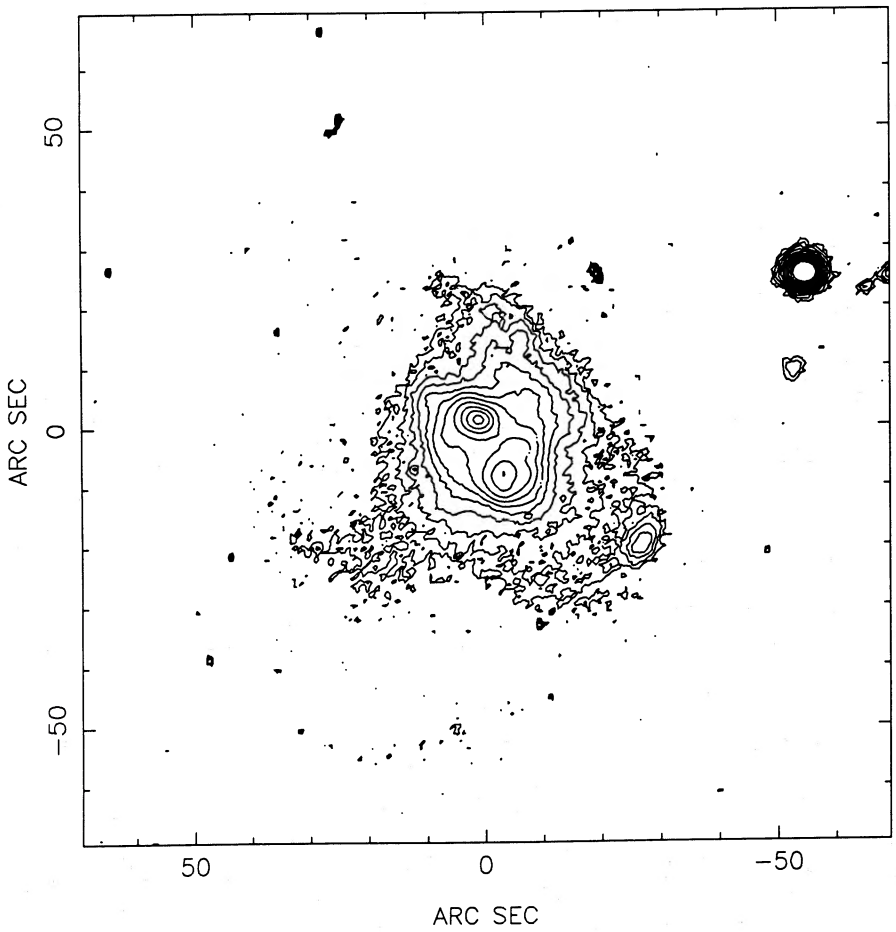

FIG. 1.—Calibrated contour diagram of Mrk 266 in the Johnson *B* band. The CCD image is a 900 s integration. Contours range from 19.5 to 24.5 mag $arcsec^{-2}$ in steps of 0.5 mag $arcsec^{-2}$. As in all images presented in this paper, north is up and east is to the left. The spatial scale on all images and contour diagrams presented here is 822 pc to 1", assuming $H_0 = 50$ km s^{-1} Mpc^{-1}.

© American Astronomical Society • Provided by the NASA Astrophysics Data System

1988ApJ...333..168M

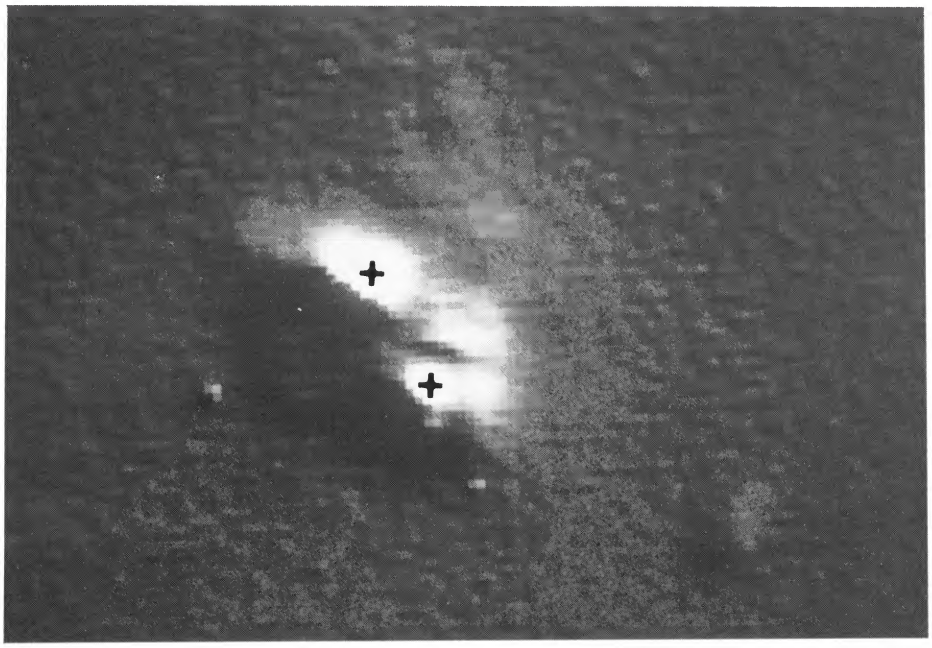

FIG. 3.—Image "derivative" obtained by measuring the differences in pixel values along the NW direction in a *B* band image. The Liner nucleus (NE) and Seyfert 2 nucleus (SW) are indicated by plus signs for scale reference and comparison with other images. Note especially the enhancement of the knots located to the west and northwest of the Seyfert 2 nucleus, and the prominent spiral or tidal feature that extends to the north.

© American Astronomical Society • Provided by the NASA Astrophysics Data System

1988ApJ...333..168M

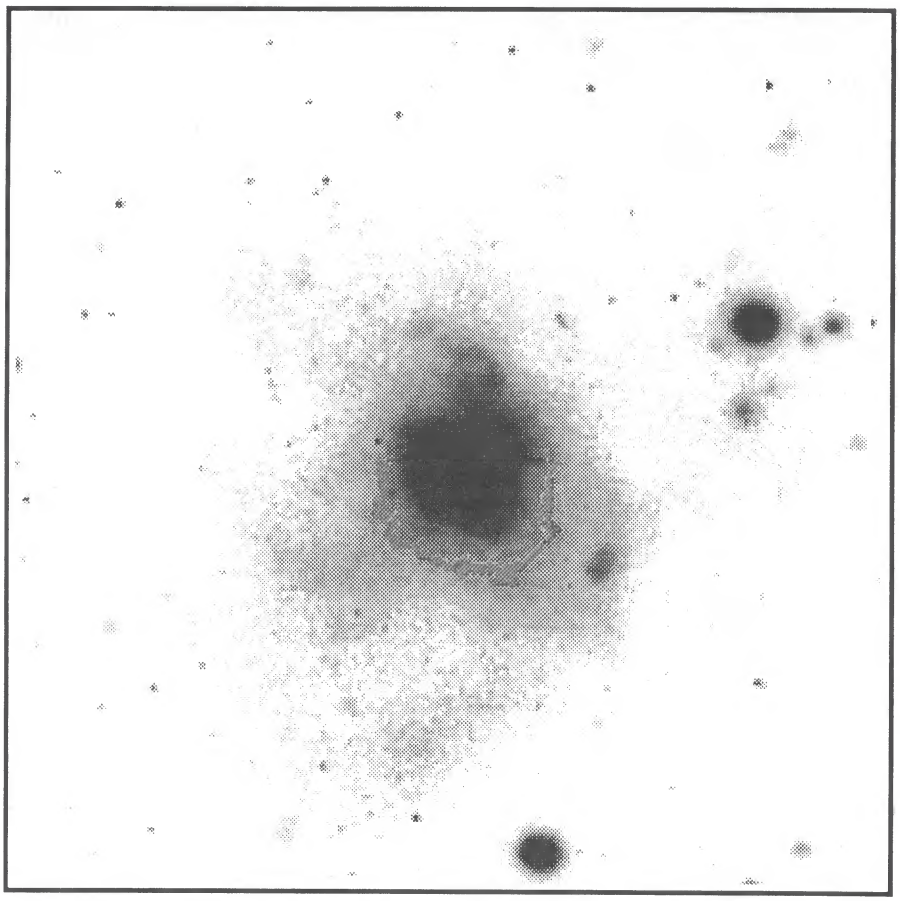

FIG. 2.—The result of co-adding four broad-band CCD images (*B*, *B*, *V*, and *R*). The total integration time is 2400 s. The angular scale can be directly determined from Fig. 1 or Fig. 6. The distance between the nuclei is 10".0. The intensity look-up table for the gray-scale image was selected to enhance the faint extended emission and tidal features in Mrk 266, as well as the double nuclei and a peculiar loop of emission that appears to terminate at a knot to the north of the nuclei.

effectively zero (Burstein and Heiles 1984). Previous photometric data available for Mrk 266 include *UBVR* measurements obtained by Huchra (1977) and near-infrared photometry reported by Allen (1976).

In an effort to detect a possible optical counterpart to the radio component located between the optical nuclei (see § III), an Hα image of Mrk 266 was obtained using the 1.3 m telescope of the McGraw-Hill Observatory on 1987 August 16. Narrow-band images (FWHM ≈ 100 Å) were obtained using filters centered near redshifted Hα + [N II] (6700 Å), and off Hα + [N II] (6600 Å). One 1200 s integration was obtained with each filter. The Hα images were reduced in approximately the same fashion as outlined above for the broad-band images. Differences in the Hα image reduction included (*a*) the use of twilight flats and (*b*) normalization of the continuum in both images using observations of a known continuum source (foreground star). After the initial reductions, the images were registered to within ±0.1 pixel and the continuum frame was subtracted from the frame containing continuum plus Hα emission. The resulting image, containing only Hα + [N II] emission, is displayed in Figure 4. In addition to the Hα emission associated with the nuclei and the northern tidal feature, we point out the presence of an apparent H II region coincident with the extranuclear knot located to 3" (2.5 kpc) the west of the Seyfert nucleus, which was noted earlier in the broad-band derivative image (Fig. 3). The ridge of H II regions to the north of the Seyfert 2 nucleus is spatially coincident with the linear feature noted in the broad-band images. Extending to the east from the Seyfert nucleus, and then curving to the southeast, is a ridge of Hα emission

TABLE 1

OPTICAL PROPERTIES OF MARKARIAN 266

FEATURE (1)	APERTURE DIAMETER (kpc)[a] (2)	(3)	*B* (4)	*B* − *R* (5)	M_B^a (6)
Nucleus *a* (SW, Seyfert 2)	5".0	4.1	16.92 ± 0.04	1.50 ± 0.08	−19.22
Nucleus *b* (NE, Liner)	5.0	4.1	16.52 ± 0.03	1.47 ± 0.07	−19.62
H II region SW of nuclei	8.0	6.6	19.06 ± 0.06	1.12 ± 0.10	−17.08
Total magnitude and color	80.0	65.6	14.04 ± 0.03	1.31 ± 0.07	−22.10

[a] Calculated assuming a distance of 169 Mpc.

© American Astronomical Society • Provided by the NASA Astrophysics Data System

1988ApJ...333..168M

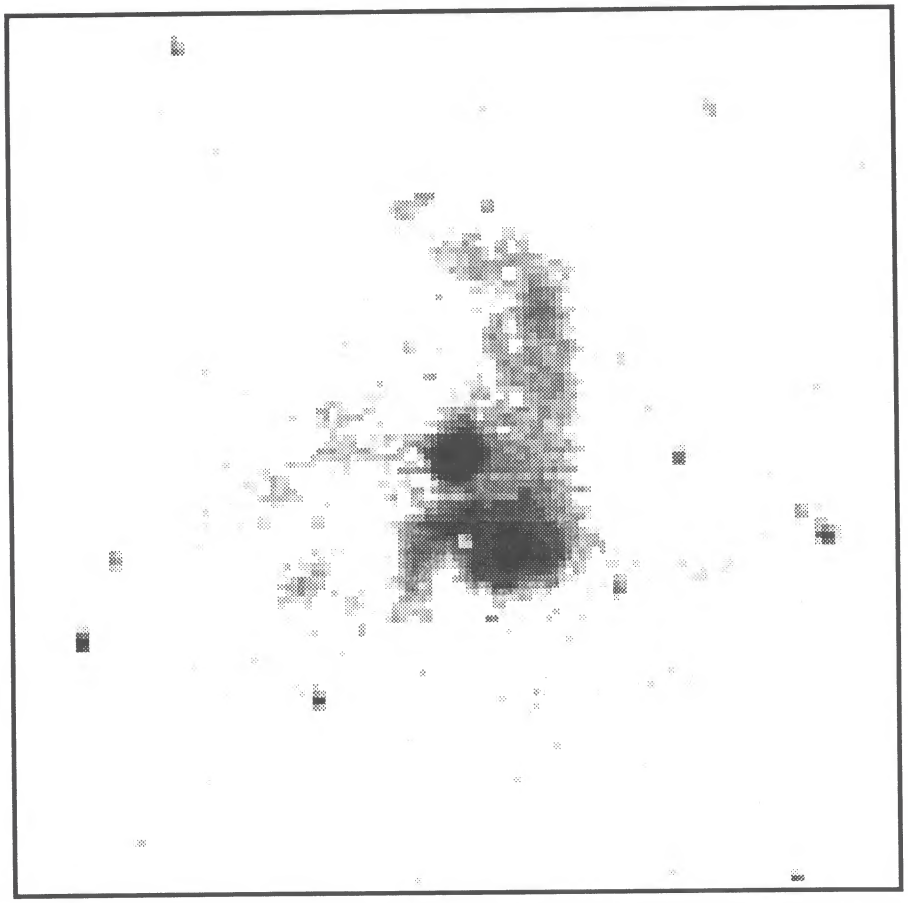

FIG. 4.—Hα + [N II] image of Mrk 266. Note the arc of Hα emission that extends northeastward from the Seyfert 2 nucleus toward the region between the active nuclei. It is not clear if these H II regions are associated with a tidal feature or a remnant spiral arm of the SW galaxy. The angular scale is clear from Fig. 5.

which maps out regions of active star formation. A contour representation of the Hα image, presented in Figure 5, clearly displays the peak to the west of the Seyfert nucleus, as well as the arcs of emission to the north and east of the Seyfert nucleus.

The optical morphology, including the double nuclei, diffuse outer halo, asymmetrical tidal features, and overall disturbed appearance, suggest that Mrk 266 is an ongoing collision/merger between two previously separate galaxies. This interpretation of the double optical nuclei and peculiar optical morphology is also supported by the presence of warm far-infrared emission. Using the *IRAS* fluxes tabulated by Lonsdale *et al.* (1985), we find $L_{60\,\mu m}/L_{100\,\mu m} = 0.61$, which is common among strongly interacting galaxies observed by *IRAS* (Young *et al.* 1986). The far-infrared luminosity of Mrk 266 is $L_{FIR} = 3.50 \times 10^{11}\ L_{\odot}$, where L_{FIR} represents the total far-infrared luminosity determined by fitting the *IRAS* 60 μm and 100 μm fluxes to a single temperature dust model as described by Lonsdale *et al.* (1985). This luminosity places Mrk 266 in the class of "high-luminosity" *IRAS* galaxies that are known to be interacting/merging systems (e.g., Lonsdale, Persson, and Mathews 1984; Sanders *et al.* 1986). Mrk 266 is also rich in molecular gas, as recently determined by CO observations which indicate that the interacting system contains a total molecular mass of $M_T(H_2) = 1.44 \times 10^{10}\ M_{\odot}$ (Sanders *et al.* 1986).

III. RADIO SYNTHESIS OBSERVATIONS

Radio synthesis observations of Mrk 266 were obtained using the Very Large Array (VLA) of the National Radio Astronomy Observatory (NRAO).[2] Approximately 1.5 hr of integration time were spent on-source in each of the A- (20 cm, 6 cm), C- (6 cm, 2 cm), and C/D- (6 cm, 2 cm) configurations during observing runs in 1987 August, February, and January, respectively. Phase calibration was performed by observing nearby point sources approximately once every 20 minutes, and an absolute flux calibration was obtained by observing the primary VLA flux calibrator, 3C 286. After initial data editing and calibration using software on the DEC-10 computer at the VLA site, further editing and CLEANing (Clark 1980) was performed using AIPS (NRAO) on the University of Michigan Astronomy VAX 11/750. Figure 6 displays contours of four co-added CCD images (*B*, *B*, *V*, and *R*) superposed on a gray-scale representation of a 20 cm continuum image. The beamwidth at 20 cm of HPBW = 1.″8 × 1.″5 provides very nearly the same resolution as the optical image (2″ seeing). These data reveal that in addition to the radio emission associated with the optical Liner and Seyfert nuclei, the NE and SW components, respectively, there is an unexpected strong radio source located *between* the active nuclei. Our detection of the radio source between the nuclei of Mrk 266 is corroborated by VLA data

[2] The National Radio Astronomy Observatory is operated by Associated Universities, Inc., under contract with the National Science Foundation.

© American Astronomical Society • Provided by the NASA Astrophysics Data System

1988ApJ...333..168M

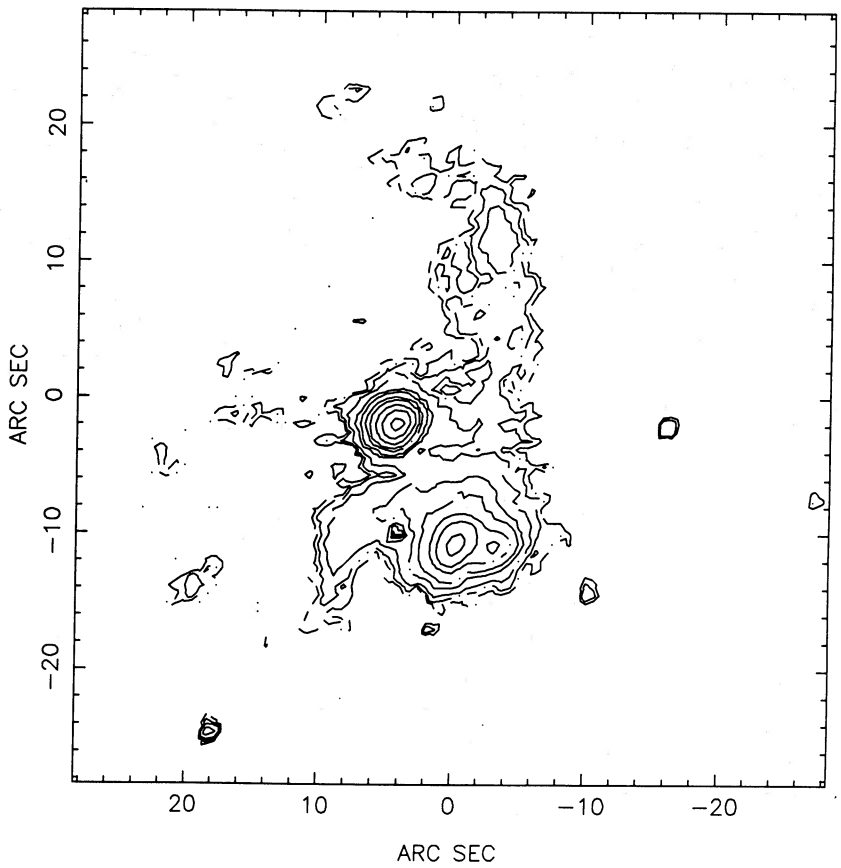

FIG. 5.—A contour diagram of the Hα + [N II] image of Mrk 266 (Fig. 4). This representation of the data clearly displays the nuclei and the peak in the Hα emission located west of the Seyfert 2 nucleus.

obtained by J. B. Hutchings (1987, private communication). There is also weak 20 cm emission associated with the northern edge of the optical (tidal?) feature found in the broad-band and Hα images. This northern emission, as well as the extended emission associated with the active nuclei, is more clearly visible in the contour diagram in Figure 7. Comparison of the contours in Figure 5 and Figure 7 indicates that the strongest Hα and 20 cm continuum emission to the north of the nuclei is associated with the conspicuous knot visible in Figure 2. Close examination of the broad-band and Hα images shows that the enhanced radio emission between the nuclei has no obvious optical counterpart with comparable morphology. It is important to note that all comparisons of optical and radio synthesis images in this paper are performed with the assumption that the peaks in the two nuclei coincide spatially. Although this is not, in general, a very safe assumption for a single peak, the fact that the separation and position angle between the nuclei of Mrk 266 are the same in the optical and radio synthesis images implies we can be highly confident in sliding the optical images to fit the more accurate VLA coordinate frame.

Additional insight into the nature of this complex system is revealed by higher resolution 6 cm observations (HPBW = 0.″3 × 0.″4) obtained using the A-configuration of the VLA in 1987 August (*see* Fig. 8). These data indicate that the central and SW radio components that were discovered with lower resolution contain complex multiple components themselves. The SW source coincident with the optical Seyfert 2 nucleus presents a "linear" morphology indicative of the double/triple continuum sources found in many Seyfert nuclei observed with the VLA (e.g., Ulvestad and Wilson 1984, and references therein). This morphology suggests that the Seyfert nucleus is transporting energy and producing radio lobes over the scale of ∼1″ (820 pc) along an axis at position angle (P.A.) −10°. The source between the optical nuclei presents a double structure (separation = 0.″4 = 320 pc) aligned along P.A. ≈ −45°, nearly normal to the axis at P.A. ≈ 30° which approximately intersects the three components separated by 5″ (4.1 kpc). Image model fitting using AIPS (NRAO) indicates that the NE radio source coincident with the optical Liner nucleus is only slightly resolved at a resolution of HPBW = 0.″3 × 0.″4.

We have used VLA observations at 20 cm (1.465 GHz), 6 cm (4.885 GHz), and 2 cm (14.962 GHz) to determine three-point spectral indices for the three radio components. The 6 cm and 2 cm maps were convolved to match the resolution of the 20 cm image (HPBW = 1.″8 × 1.″5) before flux values were measured. Table 2 lists the positions, flux densities, and three-point spectral indices, α, for the three components, where $S_\nu \approx \nu^{-\alpha}$. These results show clearly that all three components are dominated by nonthermal emission from 1.465 GHz to 14.965 GHz.

In order to evaluate the accuracy of these measurements, a discussion of the error estimates in the flux determinations is in order. Following Weiler *et al.* (1986), we have estimated the errors in the flux densities as the sum of the two major sources of measurement error, the error associated with the flux density calibration, σ_{cal}, and the "map error," σ_{map}. The calibration error results primarily from the fact that flux calibrations for measurements taken with the VLA are obtained by first "bootstrapping" the flux densities of

© American Astronomical Society • Provided by the NASA Astrophysics Data System

1988ApJ...333..168M

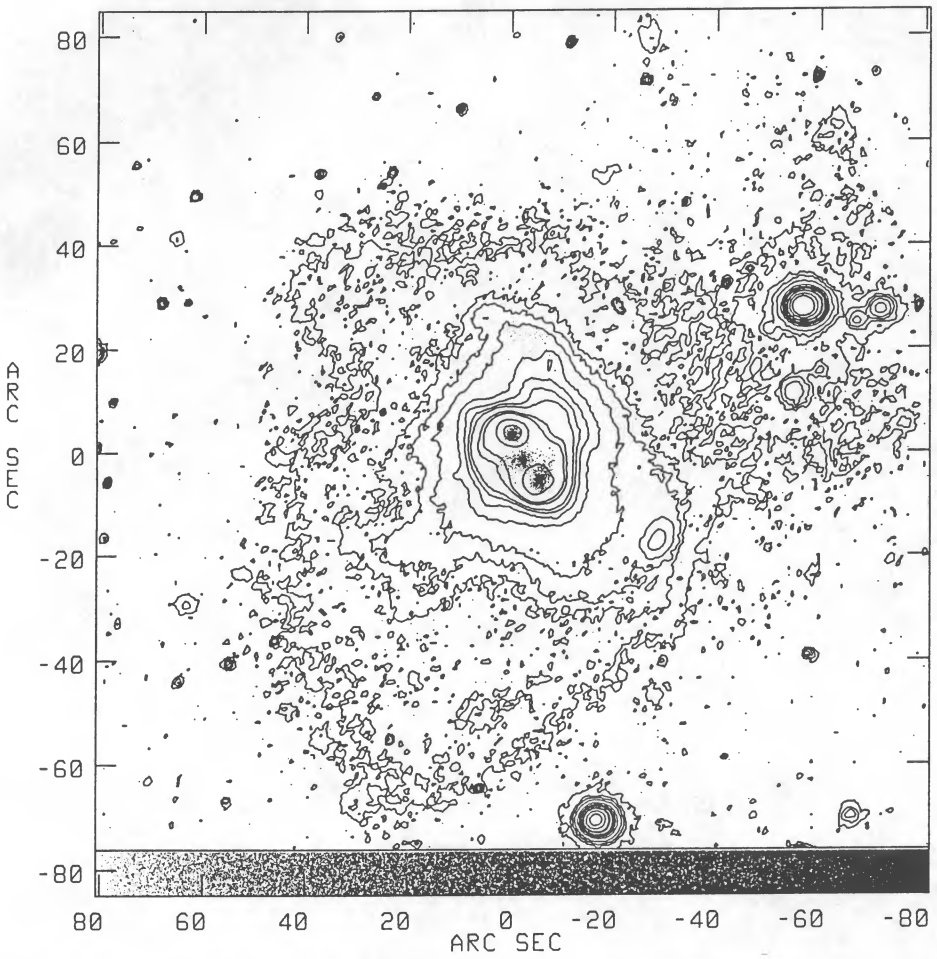

FIG. 6.—Optical contour diagram of four co-added CCD images (B, B, V, and R; 2400 s total integration) superposed on a gray-scale representation of the 20 cm VLA synthesis image. The main purpose of this diagram is to illustrate the relative positions of the three radio continuum sources with respect to the optical nuclei in Mrk 266. The morphology of the optical emission and the extent of the faint halo is also clearly represented.

secondary (phase) calibrators located near the program source from the assumed flux density of the primary flux calibrators 3C 286 and 3C 48. Then the secondary calibrators, which are observed approximately once every 15 minutes, are used to calibrate the program source. Repeated observations of a number of secondary calibrators over a long time baseline ($\sim$4 yr) have shown that in addition to secular changes which indicate variability in the secondary calibrators, random measurement errors are typically $\sim$3.5% at 20 cm and 6 cm, and $\sim$10% at 2 cm (e.g., Weiler *et al.* 1986). Lacking such numerous and long-term observations of our secondary calibrators, we have adopted these values as conservative estimates of the calibration errors in our measurements. The map error, $\sigma_{\rm map}$, is the error associated with measuring the flux density of a source from the synthesis image. Since the components of Mrk 266 have complex structure and are asymmetric, the AIPS task BLSUM was used to make repeated, independent measurements of the flux density of each component at each frequency. The errors associated with these map measurements range from $\sim$1% on the 20 cm image to 10% on the 2 cm image. A much smaller contribution to this "map error" is due to the random

TABLE 2

MEASURED RADIO PROPERTIES OF MARKARIAN 266

			S(mJy)			$P(W\ Hz^{-1})$[a]			
FEATURE (1)	α(1950) (2)	δ(1950) (3)	20 cm (4)	6 cm (5)	2 cm (6)	20 cm (7)	6 cm (8)	2 cm (9)	$\alpha^{b}_{20,6,2}$ (10)
Nucleus a (SW, Seyfert 2)	$13^h36^m13^s.75$	48°31′45″.2	32.4 ± 1.4	10.1 ± 0.5	4.9 ± 0.7	1.1×10^{23}	3.5×10^{22}	1.7×10^{22}	0.91 ± 0.04
Component between nuclei	13 36 14.79	48 31 49.1	21.5 ± 0.9	6.0 ± 0.4	2.7 ± 0.5	7.4×10^{22}	2.1×10^{22}	9.3×10^{21}	1.00 ± 0.05
Nucleus *b* (NE, Liner)	13 36 15.00	48 31 54.1	23.5 ± 1.0	12.2 ± 0.4	4.1 ± 0.6	8.1×10^{22}	4.2×10^{22}	1.4×10^{22}	0.61 ± 0.04
Northern emission	13 36 14.79	48 32 13.9	2.6 ± 0.5	...	...	8.9×10^{21}	...	...	...

[a] Power calculated assuming a distance of 169 Mpc.
[b] See text for discussion of three-point spectral index calculations and error determinations.

© American Astronomical Society • Provided by the NASA Astrophysics Data System

1988ApJ...333..168M

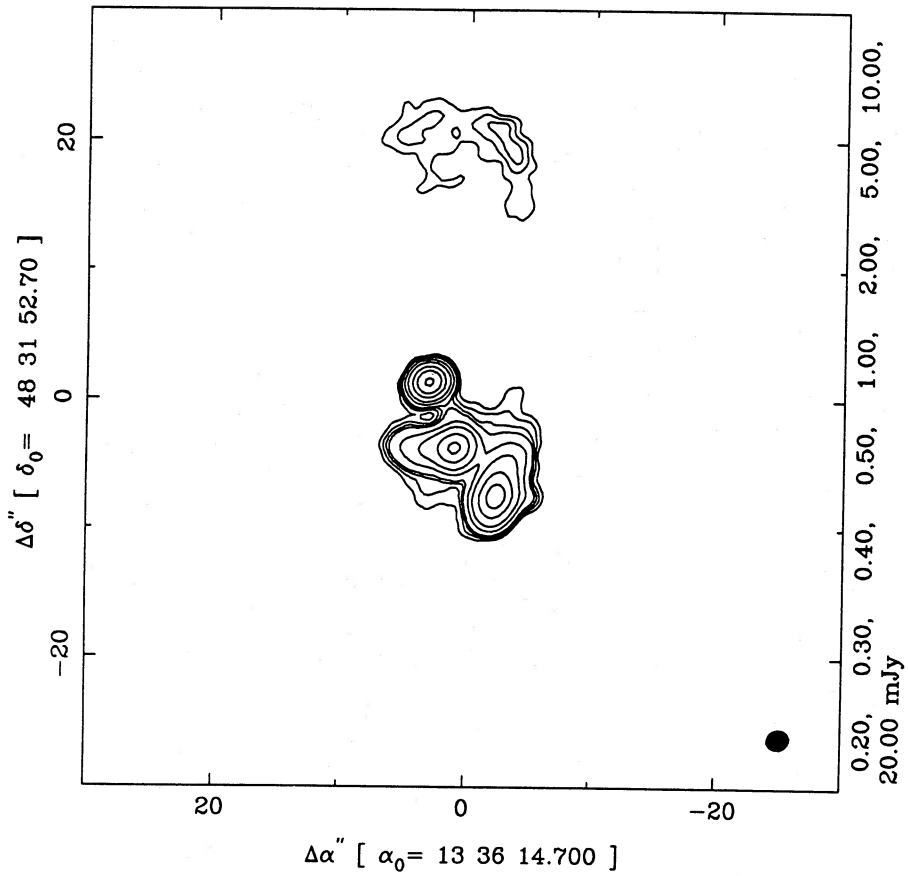

FIG. 7.—Contour diagram of A-configuration VLA 20 cm data. Sidelobes were removed with the CLEAN algorithm, and the image was mapped with natural weighting. The half-power beamwidth (HPBW) of 1".8 × 1".5 is represented by the ellipse in the lower right-hand corner of the diagram. The rms noise in the map is 0.05 mJy, and the contour levels are displayed starting at 4 times the rms noise.

fluctuations caused by receiver noise and residuals from the CLEAN process. Finally, the total error σ in each flux value listed in Table 2 is estimated to be $\sigma^2 = \sigma_{\rm cal}^2 + \sigma_{\rm map}^2$.

The total flux density of Mrk 266 at 20 cm is 80.0 ± 2.0 mJy, which corresponds to a total luminosity of 2.7×10^{23} W Hz^{-1} at the adopted distance of 169 Mpc. We obtain an integral spectral index of $\alpha = 0.85 \pm 0.05$ by summing the emission from the components at each frequency. Using 2.7 GHz, 5.0 GHz, 8.1 GHz, and 10.5 GHz flux densities of Mrk 266 obtained at various observatories, Kojoian *et al.* (1976) derived a spectral index of $\alpha = 0.62$ (±0.29), where we have estimated σ_α in their result by propagating the errors quoted in the flux densities. This at least provides a consistency check on our result for the integral spectrum.

IV. DISCUSSION

The current data suggest a number of possible interpretations for the radio emission between the nuclei of Mrk 266. After considering some alternate hypotheses, we argue that the data are most consistent with a model that involves the acceleration of cosmic rays in a shock region induced by a collision and possible ongoing merger of two galaxies.

a) Radio Lobes Produced by an Optically Obscured Central Engine?

The three strongest radio components in Mrk 266 have steep, nonthermal spectra that indicate the presence of synchrotron radiation. Triple radio morphology in Seyfert galaxies has generally been interpreted in terms of a central "engine" which transports energy into the surrounding narrow-line region (NLR), thus producing radio lobes and possibly dual optical emission-line regions (e.g., Ulvestad and Wilson 1984, and references therein). For example, triple radio structure associated with double Seyfert 2 nuclei in NGC 5929 has been interpreted in this fashion (Keel 1985). A search for optical emission-line regions associated with the radio lobes in 10 Seyfert galaxies with triple radio morphology has been recently conducted by Whittle *et al.* (1988). They find that most of the objects in their sample contain [O III] profile subcomponents which are spatially coincident with the radio lobes in the Seyfert NLRs. Are the double emission-line regions in Mrk 266, previously identified as classical Seyfert 2 and Liner nuclei, associated with radio lobes produced by material ejected from the central radio component? There are a number of facts which suggest that this is not the correct interpretation for the triple radio morphology of Mrk 266.

First, the central radio component in a Seyfert galaxy with triple radio morphology is typically coincident with the optical (stellar) nucleus of the galaxy. The radio lobes are thus located on opposite sides of the optical nucleus. This is true, for example, in Mrk 6, Mrk 34, Mrk 78, Mrk 79, Mrk 270, and Mrk 573 (Whittle *et al.* 1988, and references therein). As we have shown in § II and § III of

© American Astronomical Society • Provided by the NASA Astrophysics Data System

1988ApJ...333..168M

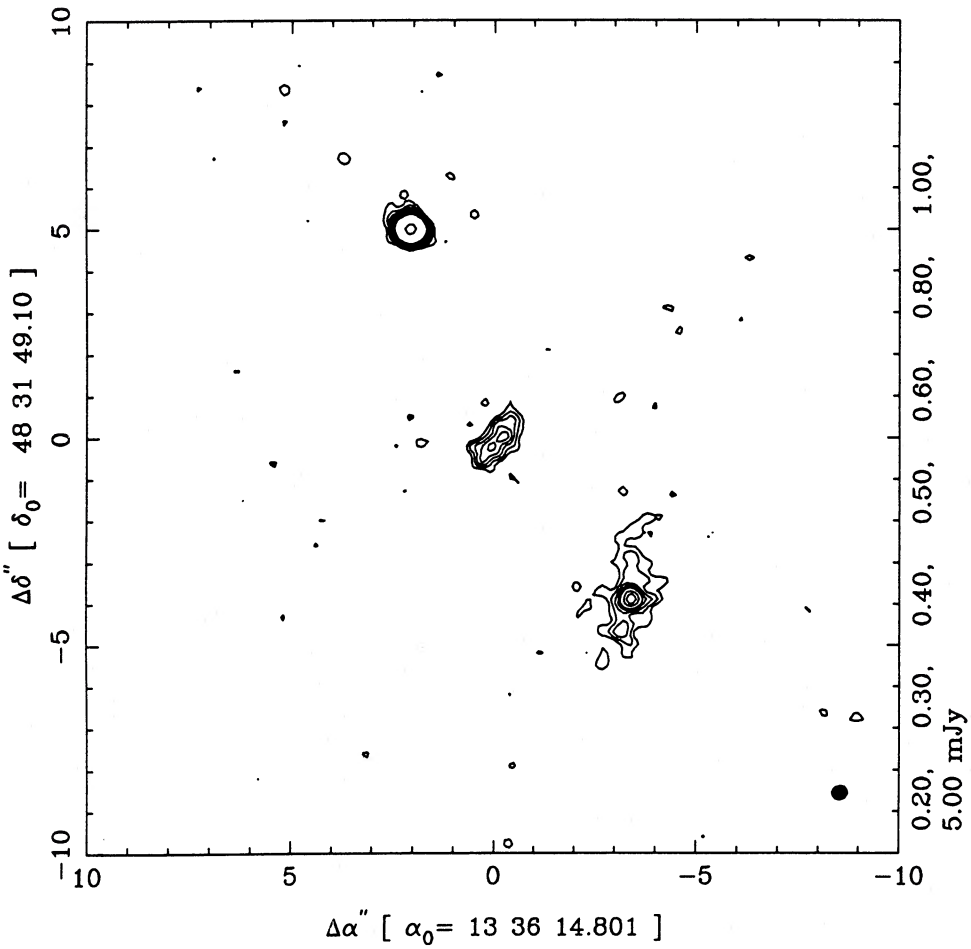

FIG. 8.—Contour diagram of C- and A-configuration VLA 6 cm data. Sidelobes were removed with the CLEAN algorithm, and the image was mapped with uniform weighting to obtain the highest possible resolution (HPBW = 0.″3 × 0.″4). The rms noise in the map is 0.07 mJy, and the contour levels are displayed starting at 3 times the rms noise.

this paper, the peak in the central radio component of Mrk 266 has no bright optical counterpart in broad-band or Hα images. Second, the higher resolution 6 cm data on Mrk 266 presented in Figure 8 provide a convincing argument against this hypothesis. The fact that the SW radio component coincident with the optical Seyfert 2 emission-line region displays a "linear" morphology much like what is observed in other Seyfert galaxies implies strongly that this object is itself producing radio lobes. The separation of the suggestive "core" and SE "lobe" in the Seyfert 2 source is 1.″0, which corresponds to 820 pc at the assumed distance of Mrk 266. We have no convincing evidence in our current data that links the radio emission between the nuclei of Mrk 266 to the ejections suggested by the "linear" morphology of the Seyfert 2 radio source. Third, we must consider the optical and far-infrared data discussed in § II which convincingly indicate that Mrk 266 consists of two galaxies that are participating in an ongoing collision and possible merger. These observations suggest strongly that the NE and SW radio components are, in fact, associated with the active nuclei of two previously separated galaxies.

These facts lead us to consider alternate explanations for the radio component between the nuclei of Mrk 266. It is appropriate to note here that there is, of course, a finite possibility that the central radio component in the VLA images of Mrk 266 is a confusing source unrelated to the interacting components of Mrk 266. However, in view of observations of enhanced radio emission between the galaxies in other interacting systems (see § IV*b* below), and the fact that the central source is resolved and exhibits an elongated geometry that possibly reflects the compression of plasma expected in a galaxy collision, we consider this possibility to be highly unlikely. For the more skeptical reader, we also point out that the *brightest* confusing source expected in the entire 3′ (FWHP) primary beam of the VLA at 2 cm is 0.1 mJy (VLA Observational Status Report, 1987 March 15). The 2 cm flux density of the radio component between the nuclei of Mrk 266 is 2.7 mJy. Thus, if the central radio component is indeed a confusing source, it is not only substantially stronger than what is expected from statistical arguments, but it is also located at an extremely fortuitous position. We now turn to a hypothesis that finds support from observations of other interacting galaxies.

b) Enhanced Radio Emission Induced by a Merger?

We have shown in § II that the optical morphology of Mrk 266 and its warm far-infrared emission as measured by *IRAS* suggest that two radio continuum sources associated with classical AGNs are in a stage of violent interaction, perhaps merging. Shocking would be expected to occur near the center of gravity of the collision, producing a burst of massive star formation and associated

© American Astronomical Society • Provided by the NASA Astrophysics Data System

1988ApJ...333..168M

supernova remnants (SNRs) which could produce the nonthermal radio emission. We have seen that although the Hα image of Mrk 266 reveals an arc of H II regions which extends eastward from the Seyfert nucleus into the region coincident with the radio emission between the nuclei of Mrk 266, the most intense star formation activity is located to the south of the peak in the central synchrotron source. It is important to note that some of the extended emission visible in the 20 cm image is spatially coincident with the eastern edge of the arc in the Hα image; however, there is not an exact spatial correspondence between the brightest H II regions and most of the extended 20 cm radiation, and the peak in the central radio component has no counterpart in either the Hα or broad-band optical images. The lack of detailed correspondence between the radio and Hα emission, in addition to the steep nonthermal spectrum of the radio emission, implies that the enhanced energy density of relativistic particles required to produce the strong radio emission between the nuclei of Mrk 266 is not produced solely by SNRs associated with the active star formation in this region. We look now to radio synthesis observations of other interacting systems which may provide an alternative hypothesis.

Numerous studies of the radio continuum emission of interacting galaxies have been performed, and some workers have been able to distinguish the emission associated with the galactic nuclei from the extended emission in the galaxies (e.g., Adams, Jensen, and Stocke 1980; Condon 1983; Hummel 1980, 1981; Stocke 1978; Stocke, Tifft, and Kaftan-Kassim 1978). A general conclusion which has emerged is that although the nuclear radio sources in some samples of interacting spiral galaxies are typically a factor of 2–3 times more luminous than the nuclei of isolated spiral galaxies, the effects of an interaction on the extended emission is generally less extreme. However, studies of very close pairs and merger candidates *do* provide some evidence that a mechanism other than fueling of the central "engine" in one or both galaxies is responsible for the enhanced radio power in these sources. We point out that although peculiar radio morphologies are not common among interacting galaxies, Mrk 266 is not unique in that other cases are known in which enhanced radio emission is observed *between* interacting galaxies.

For example, using the Westerbork Telescope, Burke and Miley (1973) discovered that the strongest nonnuclear emission in the famous interacting pair NGC 4038/4039 (Arp 224 = the "Antennae") is located between the galaxies. This led them to suggest that this emission is produced by an enhancement of the magnetic field and compression of plasma induced by the interaction of the two galaxies. Higher resolution VLA observations of the Antennae performed by Hummel and van der Hulst (1986) confirmed this result, showing that the peak in the diffuse 1.465 GHz emission associated with NGC 4038/4039 is located between the two galaxies, in a region with weak or no optical emission. The spectral index of this radio emission is in the range $0.7 < \alpha < 0.8$, which is steeper than the spectra in the surrounding regions associated with blue and Hα optical emission. The strongest extranuclear radio sources in the Antennae, knots 2 and 3 in Figure 5 of Hummel and van der Hulst, have no Hα counterparts. This situation is somewhat analogous to that in Mrk 266. Using their estimates for the flux densities and rough sizes of these sources, we estimate that the 1.465 GHz surface brightnesses of knots 2 and 3 in the Antennae are ~ 0.8 mJy arcsec^{-2} and ~ 0.9 mJy arcsec^{-2}, respectively. For comparison, the 1.465 GHz radio surface brightness of the source between the nuclei of Mrk 266 is 0.57 ± 0.04 mJy arcsec^{-2}. The source of relativistic particles needed to explain the steep radio spectrum between the nuclei of the Antennae, and similarly in Mrk 266, may be either SNRs, or a population of stars older than $\sim 10^9$ yr. In the case of an old stellar population, a locally enhanced magnetic field, shocks, or both, in the interstellar medium may be all that is required to produce the synchrotron emission, alleviating the requirement for SNRs to efficiently produce cosmic rays (Hummel and van der Hulst 1986).

Another example of this type of phenomenon was discovered in Westerbork synthesis observations of an arc of 21 cm continuum emission between NGC 7319 and NGC 7318b, members of Stephan's Quintet (Allen and Hartsuiker 1972). Follow-up observations with higher resolution using the partially completed VLA by van der Hulst and Rots (1981) revealed that the arc of emission resolves into a relatively compact structure at the SE interface between NGC 7318b and NGC 7319, and more diffuse emission displaced to the SW of the outlying spiral arm in NGC 7318b. For comparison with Mrk 266, we note that the peaks in the ridge of radio continuum emission between NGC 7318b and NGC 7319 are not spatially coincident with the bright H II regions in the nearby spriral arm, and the overall spectrum of the radio emission is nonthermal. Enhanced, nonnuclear radio continuum emission has also been attributed to a collision between two disk galaxies in the peculiar system NGC 6240 (Fosbury and Wall 1979). The purpose of this discussion is to emphasize that although the radio component between the nuclei of Mrk 266 has a unique morphology, the fact that its radio surface brightness and steep spectral index are comparable with those in these other interacting systems, along with the similar lack of an obvious optical counterpart, suggests that the radio emission is indeed related to the interaction/merger occurring in Mrk 266.

The lack of a spatially coincident broad-band or Hα counterpart to the central radio component in Mrk 266 suggests two possibilities in view of these observations of other interacting systems. The first possibility, suggested by van der Hulst and Rots (1981) in the case of Stephan's Quintet, is that the optical tracers of the burst of star formation (O stars and H II regions) expected to be associated with the interaction may have simply disappeared in this region. This is quite reasonable, since the lifetimes of massive O stars that dominate in such star bursts are only a few times 10^7 yr. Alternatively, we propose that a process first quantified by Bell (1978*a*, *b*) is taking place, in which a significant fraction of the energy produced in a shock goes into accelerating charged particles to relativistic energies. In this scenario, supersonic streaming of material produces a shock front near the interface of the gaseous disks of the colliding/merging galaxies in Mrk 266, where the mean plasma velocity changes. A qualitative outline of the particle acceleration mechanism is as follows. The shock front produces appreciable numbers of protons and electrons in the high-energy portion of their energy distributions that are able to cross the shock front into the upstream region. In the upstream region, the fast particles back-scatter off self-generated Alfvén waves, confining the particles between the regions downstream and upstream of the shock, and reducing their streaming to about the Alfvén speed. The particles are soon overtaken by the shock. Finding themselves in a region of plasma turbulence downstream, they are forward-scattered back upstream. In this fashion, energetic particles can cross the shock front many times, increasing their energies with each cycle. The resulting particle energy spectrum is a power law with an index similar to that observed for Galactic cosmic rays. Synchrotron radio emission is produced by the energetic electrons in the shocked gas, which can explain the steep spectra observed in SNRs and other radio sources where such shocking is known to occur. We point out that although this cosmic-ray acceleration mechanism was suggested independently by Axford, Leer, and Skadron

© American Astronomical Society • Provided by the NASA Astrophysics Data System

1988ApJ...333..168M

(1977), Krymsky (1977), Bell (1978*a*, *b*), and Blandford and Ostriker (1978), it was Bell who put it into quantitative terms useful for our analysis.

Using this model, we can estimate the radio power expected from the (proposed) shocked gas in the region between the nuclei of Mrk 266. The emissivity of the shocked gas is given by equation (11) in Bell (1978*b*),

$$\epsilon(\nu) = 2.94 \times 10^{-34}(1.435 \times 10^{5})^{0.75-\alpha}\xi(2\alpha+1)\left(\frac{\phi_e}{10^{-3}}\right)\left(\frac{n_e}{\text{cm}^{-3}}\right)\left(\frac{\psi_e}{4}\right)^{2\alpha}\left(\frac{\alpha}{0.75}\right)$$
$$\times\left(\frac{v_s}{10^4\ \text{km s}^{-1}}\right)^{4\alpha}\left(\frac{B}{10^{-4}\ \text{G}}\right)^{\alpha+1}\left[1+\left(\frac{\psi_e}{4}\right)^{-1}\left(\frac{v_s}{7000\ \text{km s}^{-1}}\right)^{-2}\right]^{\alpha}\left(\frac{\nu}{\text{GHz}}\right)^{-\alpha} \quad (W\ \text{Hz}^{-1}\ \text{m}^{-3}), \tag{1}$$

where B is the magnetic field of the emitting region, $\alpha = \frac{1}{2}(\mu - 1)$ is the spectral index of the radio emission, $\xi(\mu) = 11.7a(\mu)$, where $a(\mu)$ is a weak function of μ tabulated by Ginzburg and Syrovatskii (1965), n_e is the downstream electron number density, v_s is the shock velocity, ν is the radio frequency, and ϕ_e and ψ_e are defined such that the fraction ϕ_e of available electrons are injected into the shock with energies of $\psi_e(\frac{1}{2}m_p v_s^2)$. Thus the number density of particles in the accelerated particle spectrum is $\sim\phi_e n_e$.

We will calculate the expected power at 20 cm (1.465 GHz) using derived and estimated quantities from the current data on Mrk 266. Following Bell (1978*b*), who was guided by observations of the Earth's bow shock, we assume $\psi_e = 4$. Using the measured quantities listed in Table 2, we perform an equipartition calculation in which the energy in relativistic particles is required to be equal to that in the magnetic field, assuming we are observing an optically thin synchrotron source. The dimensions of the central radio source on the 20 cm synthesis image (Fig. 7) are $\sim 3''.5 \times 7''.3$, or 2.9 kpc $\times$ 6.0 kpc at a distance of 169 Mpc. Estimating the line-of-sight dimension to be simply the average of these two values (4.5 kpc) gives an approximate volume of 2.4×10^{60} m^3 for the central source. The results of the equipartition calculation for the central radio component in Mrk 266, in addition to the input parameters for the calculation, are listed in Table 3. The derived quantities directly relevant to equation (1) are the magnetic field, 2.7×10^{-4} G, and the number density of electrons producing the synchrotron spectrum, 1.1×10^{-3} cm^{-3}, which we use as an estimate of $\phi_e n_e$. The parameter with the most certainty in this calculation is the spectral index of the emission in the region between the nuclei of Mrk 266. The flux values at 20 cm, 6 cm, and 2 cm obtained from the VLA data are consistent with a spectral index of $\alpha = 1.00 \pm 0.05$. For $\alpha = 1.00$ ($\mu = 3.0$), $a(\mu) \approx 0.0742$ (Ginzburg and Syrovatskii 1965). Thus, $\xi(2\alpha + 1) = 0.868$ is the appropriate value for the central component of Mrk 266.

A critical parameter in equation (1) is the shock velocity, v_s. The expected relative velocities of cloud-cloud collisions induced by the interaction of the component spiral disks in Mrk 266 provides a reasonable estimate for the shock velocity. Using measurements of optical emission lines, Petrosian *et al.* (1980) found a radial velocity difference of 127 km s^{-1} between the active nuclei of Mrk 266. The peculiar morphology of Mrk 266 makes it difficult to estimate the angle of inclination of the encounter to the line of sight. The fact that this is not a symmetric disk galaxy indicates that the ratio of a/b listed by de Vaucouleurs, de Vaucouleurs, and Corwin (1976) for NGC 5256 cannot be used to obtain a meaningful value of sin (i). In the absence of a more reliable method of measuring the inclination, we will simply use the expected inclination of a randomly chosen galaxy on the sky, sin (i) = 0.5. Thus, the nuclei have an estimated relative velocity of $\sim$250 km s^{-1} in the plane of their encounter. Lacking knowledge of the velocity field of

TABLE 3

EQUIPARTITION CALCULATION FOR THE CENTRAL RADIO COMPONENT OF MARKARIAN 266

Parameter (1)	Value (2)	Units (3)
Input Parameters[a]		
Frequency	1465	MHz
Flux density	21.5	mJy
Spectral index	1.0	
Approximate volume	82.3	kpc^3
Distance	169	Mpc
Low-frequency cutoff	10^{-3}	MHz
$\gamma_{\text{protons}}/\gamma_{\text{electrons}}$	500	
Equipartition Calculation Results		
Equipartition magnetic field	2.7×10^{-4}	G
Field energy density	2.8×10^{-9}	ergs cm^{-3}
Particle energy density	3.7×10^{-9}	ergs cm^{-3}
Particle pressure	1.2×10^{-11}	dyne cm^{-3}
Summed energy density	6.5×10^{-9}	ergs cm^{-3}
Total source energy	1.6×10^{58}	ergs
Emission Lorentz factor	2.6×10^{3}	
Cutoff Lorentz factor	2.1	
Number density of spectrum electrons	1.1×10^{-3}	cm^{-3}
Total number of spectrum electrons	2.6×10^{63}	
Emitting electron lifetime	1.6×10^{5}	yr

[a] See text for discussion of the input parameters and their influence on equipartition results.

© American Astronomical Society • Provided by the NASA Astrophysics Data System

1988ApJ...333..168M

interstellar clouds near the interface of the colliding disks, we will assume that the interstellar material in the disks of the component galaxies are colliding at roughly this same relative speed. Thus, we will adopt a shock velocity of $v_s = 250\,\mathrm{km\,s^{-1}}$.

Substituting these observed and derived parameters into equation (1) results in a monochromatic emissivity of $\epsilon_{1.465\,\mathrm{GHz}} = 2.9 \times 10^{-38} W\ \mathrm{Hz^{-1}\ m^{-3}}$. Therefore, the predicted monochromatic power of the central radio component using Bell's electron acceleration mechanism is $P^{\mathrm{shock}}_{1.465\,\mathrm{GHz}} = 7.1 \times 10^{22} W\ \mathrm{Hz^{-1}}$. The integrated flux-density of the central radio component is $S_{1.465\,\mathrm{GHz}} = 21.5$ mJy. At a distance of 169 Mpc, this corresponds to an observed power of $P^{\mathrm{obs}}_{1.465\,\mathrm{GHz}} = 7.4 \times 10^{22} W\ \mathrm{Hz^{-1}}$. Considering the large uncertainty in the shock velocity, with the strong dependence of $v_s^{4\alpha}$ in equation (1), and the uncertainty in the volume of the relevant emission region, the agreement between the observed and theoretical powers in the central component of Mrk 266 is well within the experimental errors. Detailed measurements of the velocity field in the region between the nuclei of Mrk 266 are needed to place better contraints on this model.

In order to further evaluate how well the model predicts the radio power from the central source in Mrk 266, it is appropriate to consider the sensitivity of the emissivity computed from equation (1) to the choice of input parameters for the equipartition calculation. The least well known input parameters in the calculation are the low-frequency cutoff, ν_0, and the ratio of the energy in heavy particles to the energy in electrons, γ_p/γ_e. We have selected these parameters by systematically varying ν_0 and γ_p/γ_e, searching for combinations that provide the magnetic field and number density of spectrum electrons needed to match the emissivity from equation (1) to the observed power. With no *a priori* reason to neglect the particles accelerated only to slightly relativistic energies by Bell's mechanism, a resulting cutoff Lorentz factor of ~ 1 indicates the lower limit of ν_0 that is acceptable. The cutoff Lorentz factor is of order 1 with ν_0 in the range 10^{-4}–10^{-2} MHz. Interestingly, it is only in the region of low cutoff frequency (10^{-4}–10^{-2} MHz) and high γ_p/γ_e (200–1000) that the combination of relatively high magnetic field ($B \approx 10^{-4}$ G) and high electron density ($n_e \approx 10^{-3}$ cm^{-3}) required to match the observed power of the central component of Mrk 266 is attained. For example, at any selected ratio of γ_p/γ_e, say 100, changing ν_0 from 1 kHz to 1 MHz decreases the magnetic field by a factor of ~ 4, and decreases n_e by a factor of ~ 2800, with a resulting drop in the emissivity from equation (1) that amounts to a factor of 4×10^4. At a given cutoff frequency, increasing γ_p/γ_e from 0 to 1000 increases B by a factor of ~ 7 and increases n_e by a factor of ~ 135, resulting in a factor of $\sim 7 \times 10^3$ increase in the emissivity from Bell's mechanism. In summary, without observational constraints on the cutoff frequency and an accurate estimate for the ratio of proton to electron energies in astrophysical sources, making reasonable choices for ν_0 and γ_p/γ_e, it is possible for Bell's mechanism to under predict or over predict the radio emission of the source by at least one order of magnitude. The purpose of this analysis is to show that while the physical parameters required to verify the model are too poorly known at this time, and the situation is probably much more complex than the single shock region assumed here, the current data are certainly consistent with a model that assumes shocking is being induced by the collision/merger of the component galaxies in Mrk 266.

The results of the equipartition calculation (Table 3) indicate that individual electrons in the shock-induced, synchrotron emission region have lifetimes of only $\sim 2 \times 10^5$ yr. However, it is very important to note that this does not imply that we are witnessing such a short-lived event in the evolution of this system. It is very likely that an interpenetrating collision such as that occurring in Mrk 266 could provide enough disk material to replenish the cosmic rays that are injected into the acceleration mechanism for a period of time comparable to the dynamical time scale of the encounter or merger.

V. CONCLUSIONS

We have presented optical CCD images and multifrequency radio synthesis images of the double-nucleus galaxy Markarian 266. Our primary conclusions can be summarized as follows:

1. Broad-band CCD imaging of Mrk 266 reveals two bright nuclei separated by 8.2 kpc (10.″0) within a perturbed halo with an extent of ~ 80 kpc $\times$ 71 kpc (98″ $\times$ 86″) at a blue surface brightness of ~ 25 mag per square arcsecond. Two peculiar, asymmetric tidal features extend 15–20 kpc away from the nuclei in arcs toward the northeast and southeast of the system, and a very faint extension that extends to the SE of the outer halo is clearly visible after co-adding four broad-band images.

2. The "derivative" of a *B* band CCD image enhances two distinct extranuclear knots located to the west and northwest of the Seyfert nucleus. The knot to the northwest of the Seyfert nucleus is marginally visible on the direct *B* band images, while the knot west of the Seyfert nucleus corresponds with a distinct peak in an Hα image of Mrk 266.

3. An Hα image of Mrk 266 reveals, in addition to Hα emission associated with the Liner and Seyfert nuclei, an apparent H II region located 2.5 kpc west of the Seyfert nucleus, and ridges of Hα emission associated with spiral or tidal arms that extend outward from the Seyfert nucleus. One of these arcs of Hα emission extends eastward, toward the region between the active nuclei where a relatively strong nonthermal radio source is located. However, there is no strong Hα emission spatially coincident with the highest contour levels in the radio component between the nuclei of Mrk 266. The extended tidal features and warm far-infrared emission imply that Mrk 266 is an ongoing interaction/merger between two disk galaxies. These considerations largely rule out the suggestion of Stocke *et al.* (1978) that Mrk 266 (K388) is a distorted "dumbbell" system, which refers to two close elliptical galaxies in a common halo.

4. VLA radio synthesis images originally obtained with a resolution of $\sim 2''$ reveal the presence of a relatively strong radio continuum source located between the bright optical nuclei of Mrk 266. The active nuclei and the unexpected central radio source are detected at 20 cm, 6 cm, and 2 cm, providing the data needed to determine spectral indices for the three components. The radio emission associated with all three components are characteristic of optically thin synchrotron sources. The three fluxes provided by the current data on the central component are consistent with a steep spectral index of $\alpha = 1.00 \pm 0.05$.

5. Higher resolution VLA synthesis data at 6 cm indicate that although the NE component associated with the optical Liner nucleus is unresolved, the component between the nuclei of Mrk 266 presents an elongated morphology with two peaks separated by ~ 330 pc (0.″4), and the SW radio component associated with the optical Seyfert 2 nucleus appears to have a double/triple morphology that suggests energy transport from the Seyfert nucleus (unresolved) is producing radio lobes over the scale of ~ 800 pc.

© American Astronomical Society • Provided by the NASA Astrophysics Data System

1988ApJ...333..168M

The elongated contours of the 6 cm emission between the nuclei of Mrk 266 suggests the possibility that compression associated with the collision of two galaxy disks has influenced the geometry of the emitting region.

6. The high-resolution radio synthesis image, combined with the optical broad-band and Hα images, provide important information for distinguishing between a number of possible interpretations of the triple radio structure originally discovered with 2″-resolution VLA synthesis images. We propose that the enhanced radio emission between the nuclei of Mrk 266 is produced by synchrotron emission stimulated by the collision of two galaxies. Cloud-cloud collisions induced by the ongoing merger of two disk galaxies may accelerate cosmic rays and locally enhance the magnetic field in the region between the nuclei where compression and shocking is most intense. This particle acceleration mechanism, first quantified by Bell (1978*a*, *b*), and applied to the peculiar galaxy NGC 6240 by Fosbury and Wall (1979), can consistently explain the power and spectrum observed for the radio emission between the nuclei of Mrk 266. These results imply that we are witnessing a relatively short-lived phase in the evolution of this system.

7. We have noted that there is, of course, a finite possibility that the central radio component in the VLA images of Mrk 266 is a confusing source unrelated to the interacting components of Mrk 266. However, in view of the consistency of the shock model outlined above, the observations of somewhat similar emission between galaxies in other interacting systems, and consideration of VLA confusion statistics, we consider this possibility to be highly unlikely.

A more general implication which may be implied by these results is that shocking induced by a collision or merger in other peculiar systems such as Mrk 266 may be a primary mechanism responsible for the findings of Stocke (1978) and Heckman (1983) that close galaxy pairs and mergers are ~2–8 times more likely to be radio-loud than galaxies in other samples. The important role of galaxy collisions and mergers in the production of very powerful radio sources has also been emphasized recently by Heckman *et al.* (1986). A recent 13 cm survey of 96 non-Seyfert Markarian galaxies conducted by Dressel (1987) resulted in the perplexing finding that peculiar Markarian galaxies typically have about a 60% excess in the ratio of radio continuum flux per unit far-infrared flux as compared to other Markarian galaxies and normal spiral galaxies. Dressel pointed out that it is not clear whether this result means that interactions somehow generate enhanced nonstellar radio emission and strong magnetic fields, or that the interactions stimulate the production of a higher number of supernova progenitors than in the star bursts associated with noninteracting galaxies. Our interpretation of the enhanced radio emission between the nuclei of Mrk 266 suggests strongly that the shocks produced during close interactions and mergers between galaxies may indeed induce strong radio sources of nonstellar origin, thus providing a likely explanation for Dressel's result. Considering that the central, shock-induced component contributes 28% of the total 20 cm continuum emission from Mrk 266, it seems evident that processes other than fueling the mysterious "engines" in the nuclei of the participant galaxies, and the stimulation of massive star bursts and consequent supernova remnants, can play an important role in the production of powerful radio sources in interacting/merging galaxies. Clearly, further radio continuum synthesis imaging and optical CCD observations are needed to determine the extent of shock-induced synchrotron emission in other interacting systems. The complex nature of Mrk 266, including the likelihood of variability in its radio emission (Bieging *et al.* 1977), also warrants further investigation.

We would like to thank J. B. Hutchings for providing a VLA contour diagram which corroborates our detection of the central radio component in Mrk 266. We are grateful to W. Keel and W. J. M. van Bruegel for helpful discussions during the AGN Conference in Atlanta. The comments and suggestions of the referee were extremely helpful. The assistance of R. Barr and M. Johns at the McGraw-Hill Observatory is greatly appreciated, as well as help we received from the staff of the National Radio Astronomy Observatory's Very Large Array. Special thanks goes to the rancher in Dusty who kindly helped a tired astronomer navigate back toward civilization. J. M. M. was supported during this work, in part, by a Rackham Dissertation/Thesis Grant from the University of Michigan. This research was supported in part by NSF grant AST 85-01093.

REFERENCES

Adams, M. T., Jensen, E. B., and Stocke, J. T. 1980, *A.J.*, **85**, 1010.
Allen, D. A. 1976, *Ap. J.*, **207**, 367.
Allen, R. J., and Hartsuiker, J. W. 1972, *Nature*, **239**, 324.
Axford, W. I., Leer, E., and Skadron, G. 1977, in *Proc. 15th Internat. Cosmic Ray Conf.* (Plovdiv: Bulgaria), Vol. **2**, p. 273.
Bailey, J. A., and Pooley, G. G. 1968, *M.N.R.A.S.*, **138**, 51.
Bell, A. R. 1978*a*, *M.N.R.A.S.*, **182**, 147.
———. 1978*b*, *M.N.R.A.S.*, **182**, 443.
Bieging, J. H., Biermann, P., Fricke, K., Pauliny-Toth, I. I. K., and Witzel, A. 1977, *Astr. Ap.*, **60**, 353.
Blandford, R. D., and Ostriker, J. P. 1978, *Ap. J.* (*Letters*), **221**, L29.
Burke, B. F., and Miley, G. K. 1973, *Astr. Ap.*, **28**, 379.
Burstein, D., and Heiles, C. 1984, *Ap. J. Suppl.*, **54**, 33.
Clark, B. 1980, *A.J.*, **89**, 355.
Condon, J. J. 1983, *Ap. J. Suppl.*, **53**, 459.
de Vaucouleurs, G., de Vaucouleurs, A., and Corwin, H. G. 1976, *Second Reference Catalogue of Bright Galaxies* (Austin: University of Texas Press).
Dixon, R. S. 1970, *Ap. J. Suppl.*, **20**, 2.
Dressel, L. L. 1987, in *Star Formation in Galaxies*, ed. C. J. Lonsdale Persson (NASA CP-2466), p. 579.
Fosbury, R. A. E., and Wall, J. V. 1979, *M.N.R.A.S.*, **189**, 79.
Ginzburg, V. L., and Syrovatskii, S. I. 1965, *Ann. Rev. Astr. Ap.*, **3**, 297.
Heckman, T. M. 1983, *Ap. J.*, **268**, 628.
Heckman, T. M., Smith, E. P., Baum, S. A., van Breugel, W. J. M., Miley, G. K., Illingworth, G. D., Bothun, G. D., and Balick, B. 1986, *Ap. J.*, **311**, 526.
Huchra, J. P. 1977, *Ap. J. Suppl.*, **35**, 171.
Hummel, E. 1980, *Astr. Ap. Suppl.*, **41**, 151.
———. 1981, *Astr. Ap.*, **96**, 111.
Hummel, E., and van der Hulst, J. M. 1986, *Astr. Ap.*, **155**, 151.
Karachentsev, I. D. 1972, *Catalog of Isolated Pairs of Galaxies in the Northern Hemisphere* (*Comm. Spec. Astr. Obs. USSR*, **7**, 3).
Keel, W. C. 1985, *Nature*, **318**, 43.
Kojoian, G., Sramek, R. A., Dickinson, D. F., Tovmassian, H., and Purton, C. R. 1976, *Ap. J.*, **203**, 323.
Kollatschny, W., and Fricke, K. J. 1984, *Astr. Ap.*, **135**, 171.
Krymsky, G. F. 1977, *Dokl. Akad. Nauk. SSSR*, **234**, 1306.
Landolt, A. U. 1983, *A.J.*, **88**, 439.
Lonsdale, C. J., Helou, G., Good, J. C., and Rice, W. L. 1985, *Cataloged Galaxies and Quasars Observed in the IRAS Survey* (Washington, DC: US Government Printing Office).
Lonsdale, C. J., Persson, S. E., and Mathews, K. 1984, *Ap. J.*, **287**, 95.
Osterbrock, D., and Dahari, O. 1983, *Ap. J.*, **273**, 478.
Petrosian, A. R. 1980, *Astrofizika*, **16**, 631.
Petrosian, A. R., Saakian, K. A., and Khachikian, Ye. E. 1978, *Astrofizika*, **14**, 69.
———. 1979, *Astrofizika*, **15**, 209.
———. 1980, *Astrofizika*, **16**, 621.
Sanders, D. B., Scoville, N. Z., Young, J. S., Soifer, B. T., Schloerb, F. P., Rice, W. L., and Danielson, G. E. 1986, *Ap. J.* (*Letters*), **305**, L45.
Stocke, J. T. 1978, *A.J.*, **83**, 348.
Stocke, J. T., Tifft, W. G., and Kaftan-Kassim, M. A. 1978, *A.J.*, **83**, 322.
Ulvestad, J. S., and Wilson, A. S. 1984, *Ap. J.*, **285**, 439.

© American Astronomical Society • Provided by the NASA Astrophysics Data System

1988ApJ...333..168M

van der Hulst, J. M., and Rots, A. H. 1981, *A.J.*, **86**, 1775.
Weiler, K. W., Sramek, R. A., Panagia, N., van der Hulst, J. M., and Salvati, M. 1986, *Ap. J.*, **301**, 790.
Whittle, M., Pedlar, A., Meurs, E. J. A., Unger, S. W., Axon, D. J., and Ward, M. J. 1988, *Ap. J.*, **326**, 125.
Young, J. S., Kenney, J. D., Tacconi, L., Claussen, M. J., Haung, Y.-L., Tacconi-Garman, L., Xie, S., and Schloerb, F. P. 1986, *Ap. J.* (*Letters*), **311**, L17.
Zwicky, F. 1971, *Catalogue of Selected Compact Galaxies and of Post-Eruptive Galaxies* (Guemligen, Switzerland: F. Zwicky).

H. D. ALLER, P. A. HUGHES, and J. M. MAZZARELLA: Department of Astronomy, University of Michigan, Ann Arbor, MI 48109-1090

R. A. GAUME: E. O. Hulburt Center for Space Research, Naval Research Laboratory, Code 4134 G, Washington, DC 20375-5000

© American Astronomical Society • Provided by the NASA Astrophysics Data System